

THE EFFECT OF THE CORIOLIS FORCE ON DISTAL EJECTA DEPOSITS ON MARS. K.E. Wilbur and P.H. Schultz, Department of Geological Sciences, Brown University, Box 1846, Providence, RI 02912-1846 (Kelly_Wilbur@brown.edu).

Introduction: The surface of Mars preserves a rich history of impact cratering throughout time. Due to atmospheric drag during re-entry, small ejecta from major impacts have contributed to the global layer of debris found on the surface. This is in contrast to the Moon where such ejecta would have impacted the surface to form secondary craters. The role of the atmosphere is not the only difference between the Moon and Mars. Both the rapid rotation of Mars and its small radius create force terms that become significant for large ballistic ranges.

This study describes the consequences of the Coriolis force on distal ejecta deposition on Mars. It calculates the contribution of ejecta deposits relative to a simple ejecta-thinning law on a non-rotating body. A surprising result of this study is the 17-fold increase of ejecta accumulations due to the Coriolis effect, typically found on the pole opposite the impact site. Consequently, distal clastic and melt products should provide significant contributions to deposits at high latitudes at the time of impact.

Background: Previous studies have considered trajectories on rotating bodies. Dobrovolskis [1] studied how ballistic trajectories of ejecta are affected by the Coriolis effect with application to Mercury. Alvarez et al. [2] also discussed the Coriolis effect on distal ejecta from the Chicxulub crater on Earth. More recently, other studies [3] have considered global distribution of impact melt from large oblique craters.

Lorenz [4] specifically proposed that distal microtektites should contribute to polar deposits. His model included estimates of deposit thickness values from ejecta laws for non-rotating trajectories with impact points modified by the Coriolis term.

Approach and Results: The present study traces trajectories for ejecta traversing a rotating Mars. It incorporates the ejecta-scaling model of Housen et al. [5] to map out the total contribution of ejecta to a given region on Mars. Also involved is the application of a series of detailed ballistic equations, adjusted to include the effect of rotation. Actual ejecta trajectories have been plotted on a surface projection of Mars for several different impact sites. Ejecta-scaling models were utilized to estimate deposit thickness values.

The large Hesperian-age crater Lyot (220 km in diameter) was selected to illustrate the results of this study. A direct radial decay component from Lyot to the north pole is observed (Figure 1). However, it is the direct, wrapping trajectories in the opposite hemi-

sphere that contribute a significant component of the deposits (Figure 2). Because of the complexity of these terminal trajectories and velocities, we have estimated the total contribution to the opposite high-latitude areas by selecting velocities sufficient enough to achieve latitudes poleward of approximately -60° . Ejecta velocities between the minimum velocity necessary to reach this latitude and the escape velocity (5.02 km/s for Mars) are binned in 45° quadrants and summed over this polar area. For comparison, the minimum velocity used, 3.42 km/s, is equivalent to the velocity necessary to deliver material to a distance of 1200 km from Chicxulub on Earth.

This study produced thickness values (centimeters) for direct deposits on the north pole, due to ejecta from the Lyot impact, that are comparable to the results of Lorenz [4]. However, our results showed that the opposite hemisphere would receive up to 2.5 m of deposit directly (no bulking or ablation losses assumed) followed by another 2.3 m from trajectories from the opposite direction. This contrasts with estimates by Lorenz [4] of millimeter thick deposits at the south pole.

Conclusions: The Coriolis force created by a rotating body significantly modifies the distribution of distal ejecta deposits. One ramification of this rotational effect on Mars is the concentration of ejecta on the pole of the hemisphere opposite from impact.

Although this study reinforces previous conclusions [4] that distal microtektites could be preserved in layered terrains, it also shows that earlier estimates of the thicknesses of such deposits appear to be significantly underestimated.

The next step in this study is to identify and map the cumulative contributions of ejecta deposits from specific impacts ranging in age from Amazonian to Late-Hesperian. Ejecta isopach maps should provide insight into the amount of material that has been deposited over time on the surface of Mars due to such impacts.

References: [1] Dobrovolskis A. (1981) *Icarus*, 47, 203-219. [2] Alvarez W. et al. (1995) *Science*, 269, 930-935. [3] Schultz, P.H. and Mustard, J.F. (2001) LPSC XXXII, #1668. [4] Lorenz R. D. (2000) *Icarus*, 144, 353-366. [5] Housen K.R., Schmidt R.M. and Holsapple K.A. (1983) *JGR*, 88, 2485-2499.

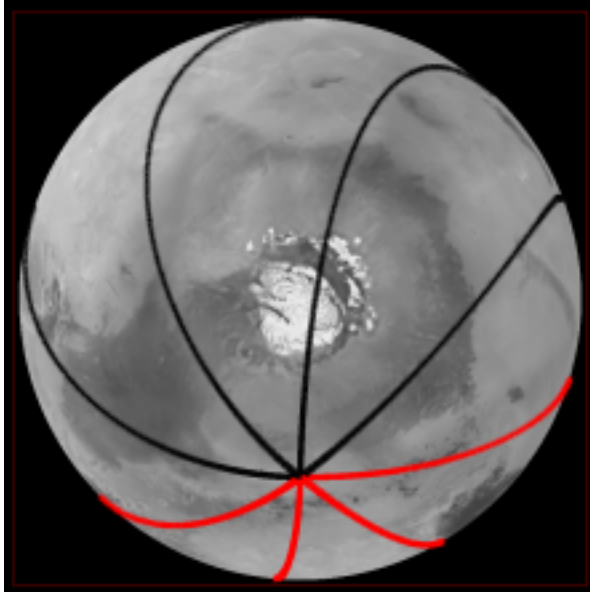


Figure 1. Orthographic projection of the northern pole of Mars. The trajectories trace the paths of ejecta launched from the Lyot impact crater site, incorporating the Coriolis effect. Due to the north pole being relatively close to the Lyot crater, the Coriolis force does not substantially affect the ejecta trajectories in this region.

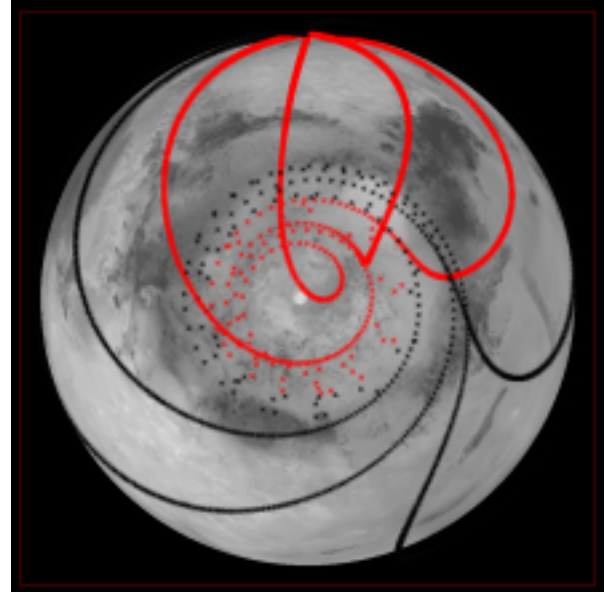


Figure 2. Lambert equal-area projection of the southern pole of Mars. The red trajectories are paths of ejecta coming directly from the impact site. The black trajectories trace ejecta paths that have wrapped around the planet, thereby arriving at the pole at a later time than the direct trajectories.

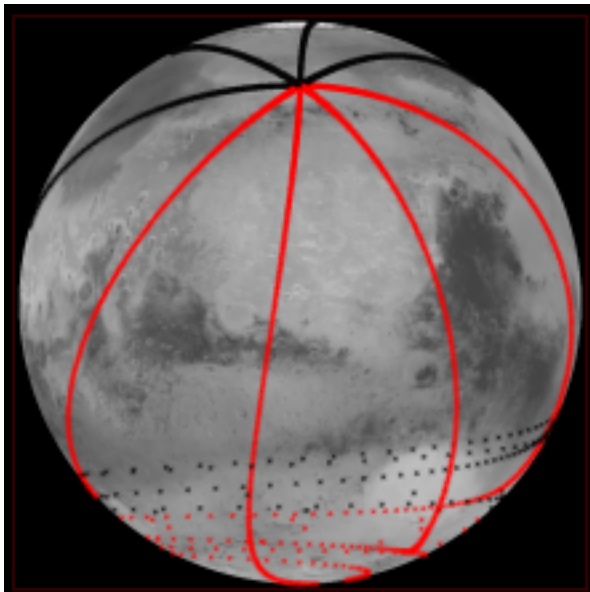


Figure 3. Orthographic projection of Mars centered at $(0^\circ, 29^\circ\text{E})$. Shown are trajectories of ejecta launched from the Lyot impact site at azimuth intervals of 45° . The effect of the Coriolis force is noticeable in the wrapping of the trajectories in the opposite hemisphere.

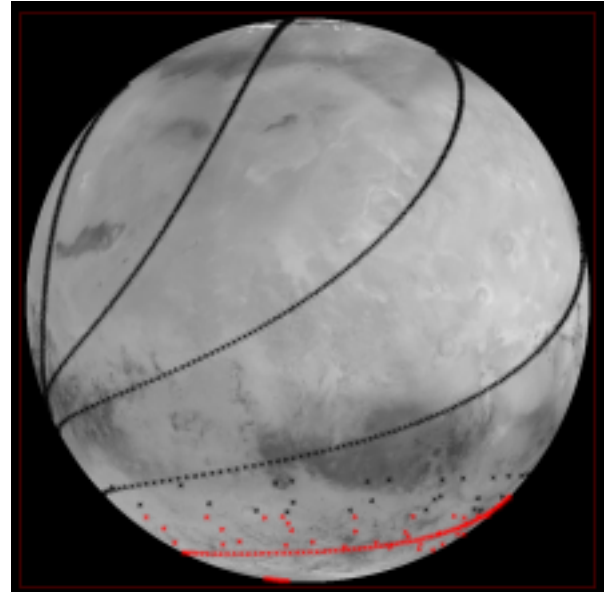


Figure 4. Companion image to Figure 3. This image is centered at $(0^\circ, 151^\circ\text{W})$, displaying the opposite hemisphere of Figure 3. Trajectories, unlike non-rotating ballistic trajectories, depart from the paths of great circles.